



MSPA-DLA++: A multi-scale phase attention deep layer aggregation for lesion detection in multi-phase CT images

Titinunt Kitrungrotsakul

Reserach Scientist
Zhejiang lab, China





Reserach motivation

- Number of deaths from liver cancer worldwide.
 - Detection
 - Segmentation
 - etc.
- Why medical imaging methods are important for healthcare?
 - High accuray
 - Reduce task and cost of medical staff
- How to utilizing medical data to bring out their potential?



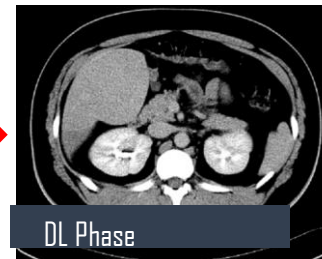
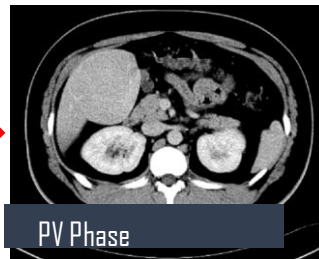
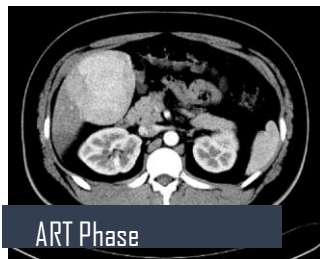
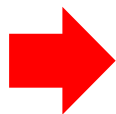
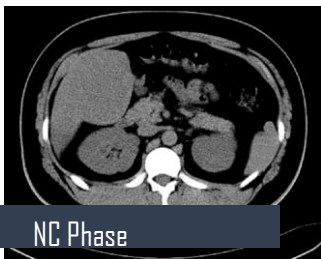
Multi-phase CT image

Before injection

30-40 s

70-80 s

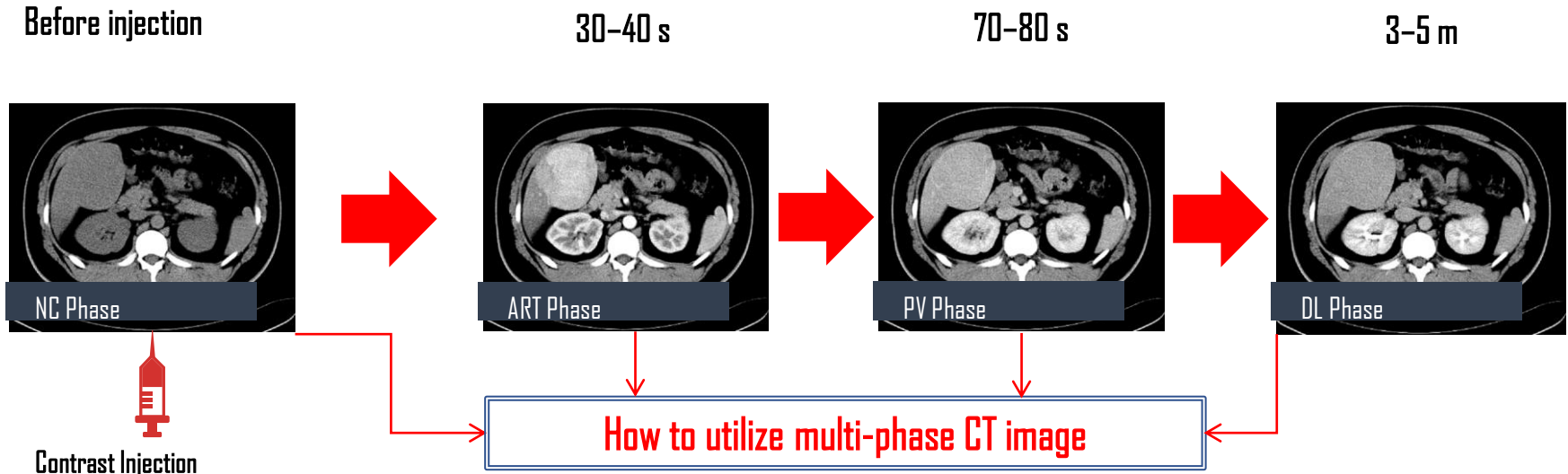
3-5 m



Contrast Injection

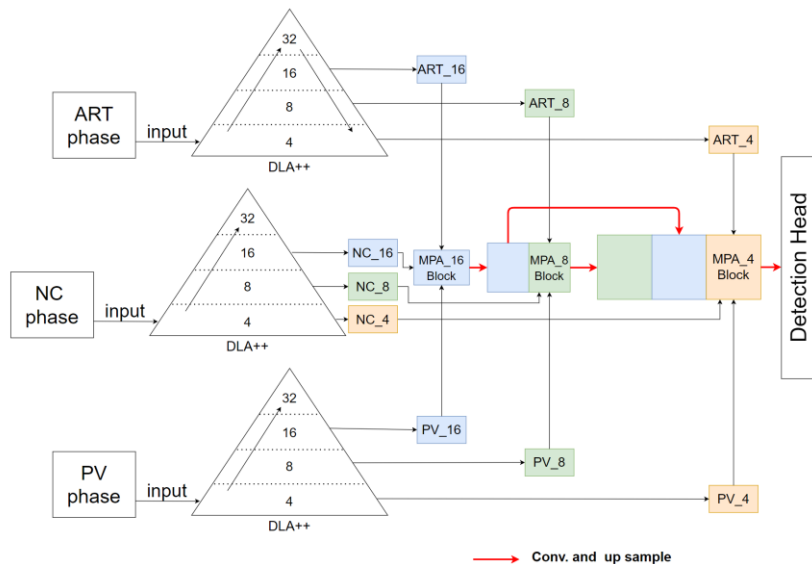


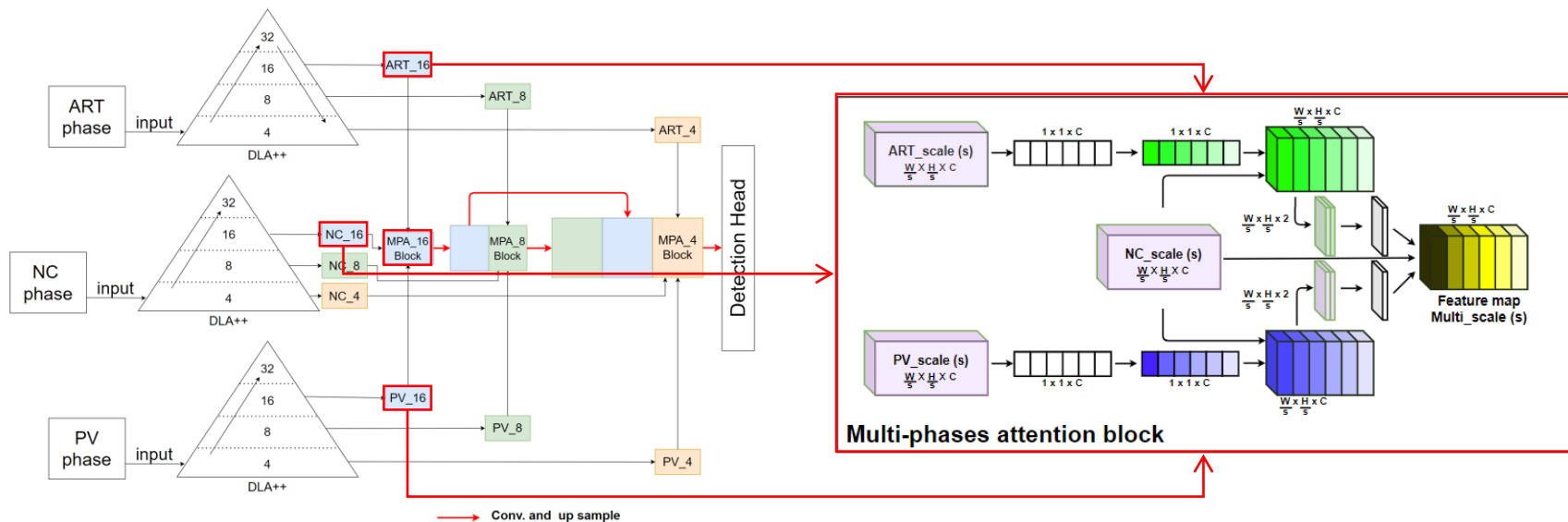
Multi-phase CT image





Architecture of MSPA-DLA++

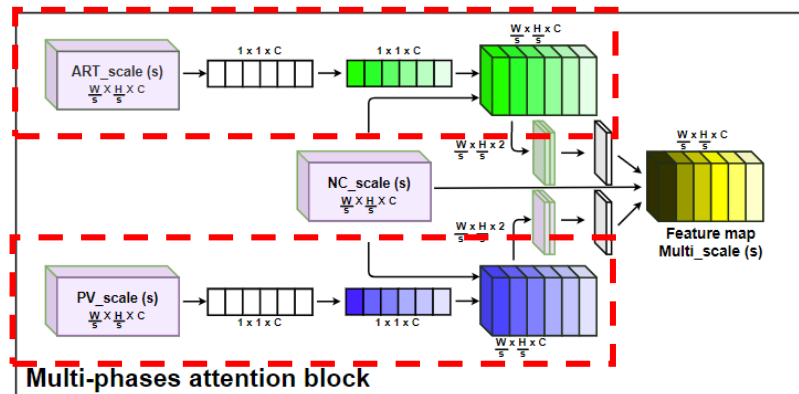






Channel attention features

$$F_{x1,x2}^{C,s} = F_{x1}^s \otimes \sigma(MLP(AvgPool(F_{x2}^s)))$$

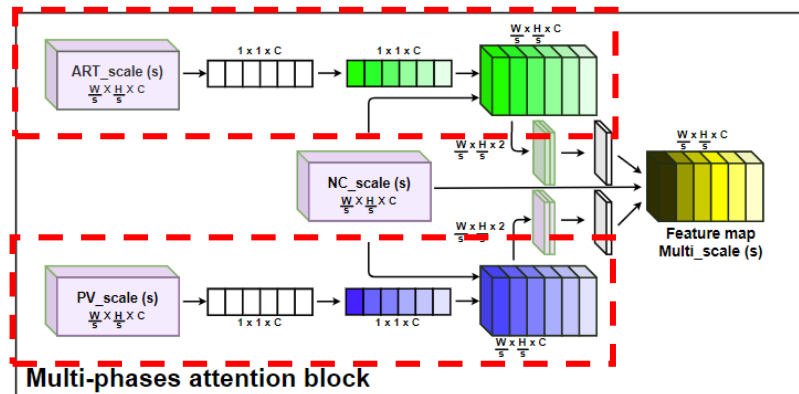




Channel attention features

$$F_{x1,x2}^{C,s} = F_{x1}^s \otimes \sigma(MLP(AvgPool(F_{x2}^s)))$$

Why only ART and PV on channel attention features extraction process?



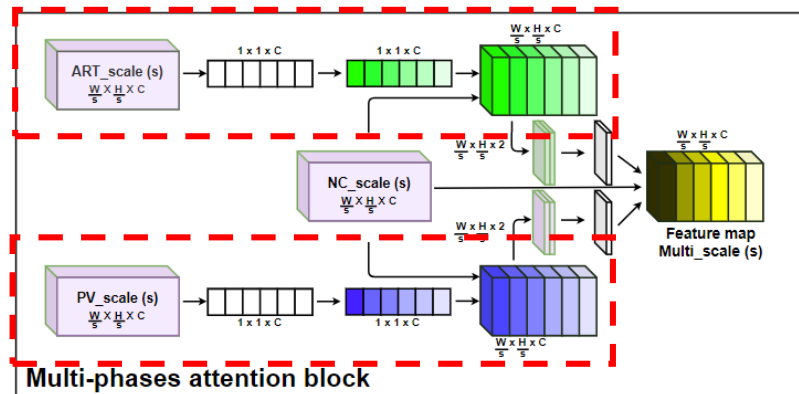


Channel attention features

$$F_{x1,x2}^{C,s} = F_{x1}^s \otimes \sigma(MLP(AvgPool(F_{x2}^s)))$$

Why only ART and PV on channel attention features extraction process?

1. NC provide unnecessary features (not important features).



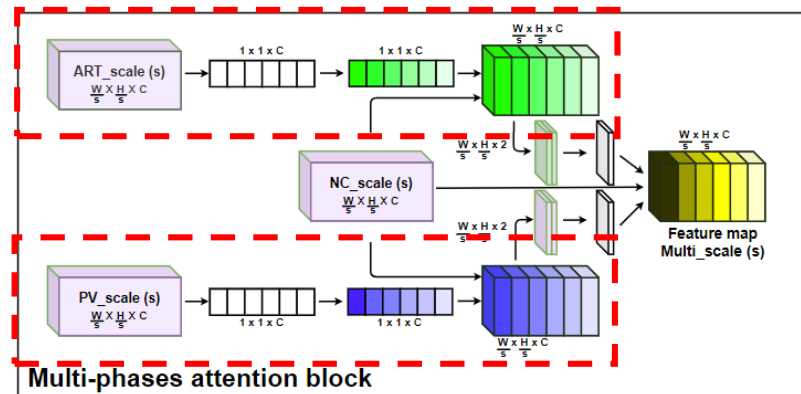


Channel attention features

$$F_{x1,x2}^{C,s} = F_{x1}^s \otimes \sigma(MLP(AvgPool(F_{x2}^s)))$$

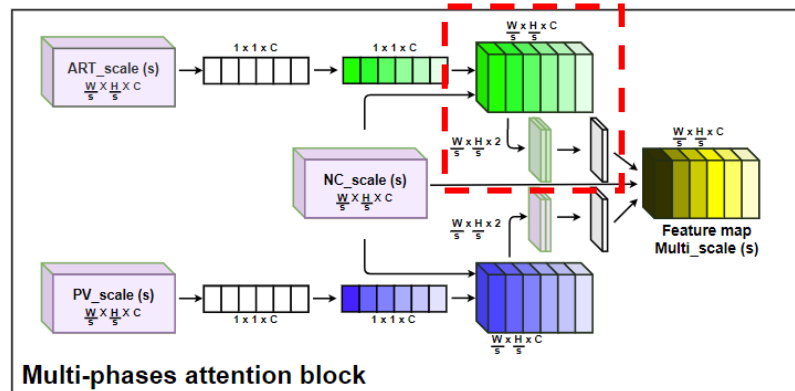
Why only ART and PV on channel attention features extraction process?

1. NC provide unnecessary features (not important features).
2. Based on our experiment w./wo. channel attention from NC make not significant improvement.





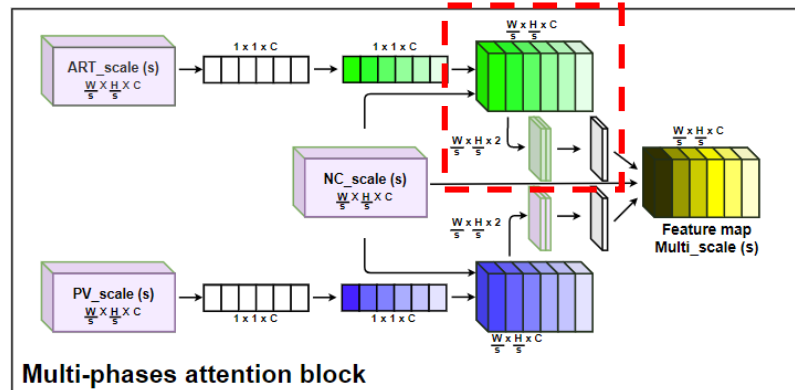
Spatial attention features





Spatial attention features

$$F_{x_1, x_2}^{S, s} = f^{7 \times 7}([\text{AvgPool}(F_{x_1, x_2}^{C, s}), \text{MaxPool}(F_{x_1, x_2}^{C, s})])$$

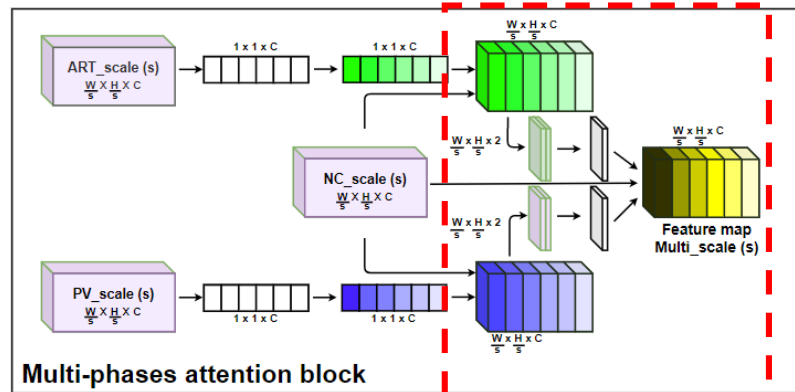




Spatial attention features

$$F_{x1,x2}^{S,s} = f^{7 \times 7}([AvgPool(F_{x1,x2}^{C,s}), MaxPool(F_{x1,x2}^{C,s})])$$

$$\hat{F}^s = F_{NC}^s \otimes \sigma(F_{NC,ART}^{S,s} + F_{NC,PV}^{S,s})$$

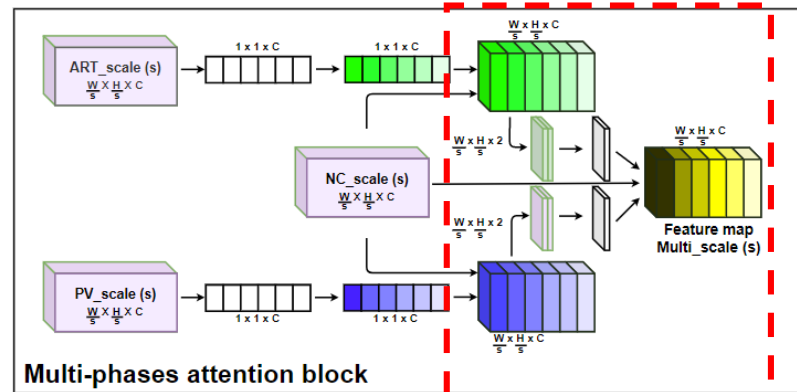




Spatial attention features

$$F_{x1,x2}^{S,s} = f^{7 \times 7}([\text{AvgPool}(F_{x1,x2}^{C,s}), \text{MaxPool}(F_{x1,x2}^{C,s})])$$

$$\hat{F}^s = F_{NC}^s \otimes \sigma(\underbrace{F_{NC,ART}^{S,s}} + \underbrace{F_{NC,PV}^{S,s}})$$



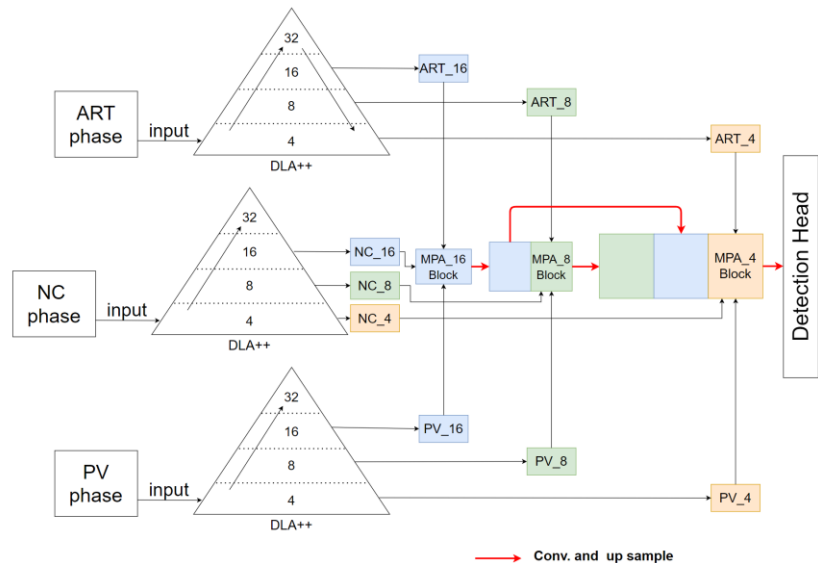


Multi-scale features

$$F_{x_1, x_2}^{S, s} = f^{7 \times 7}([\text{AvgPool}(F_{x_1, x_2}^{C, s}), \text{MaxPool}(F_{x_1, x_2}^{C, s})])$$

$$\hat{F}^s = F_{NC}^s \otimes \sigma(\underline{F_{NC, ART}^{S, s}} + \underline{F_{NC, PV}^{S, s}})$$

$$\hat{F}^2 = H(\hat{F}_{NC}^4, H(\hat{F}_{NC}^8, \hat{F}_{NC}^{16}), H(H(\hat{F}_{NC}^{16})))$$



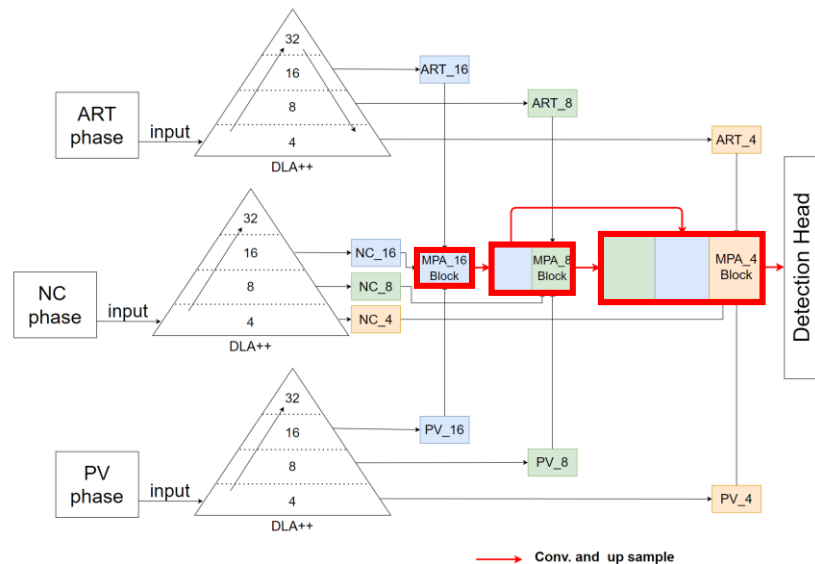


Multi-scale features

$$F_{x_1, x_2}^{S, s} = f^{7 \times 7}([\text{AvgPool}(F_{x_1, x_2}^{C, s}), \text{MaxPool}(F_{x_1, x_2}^{C, s})])$$

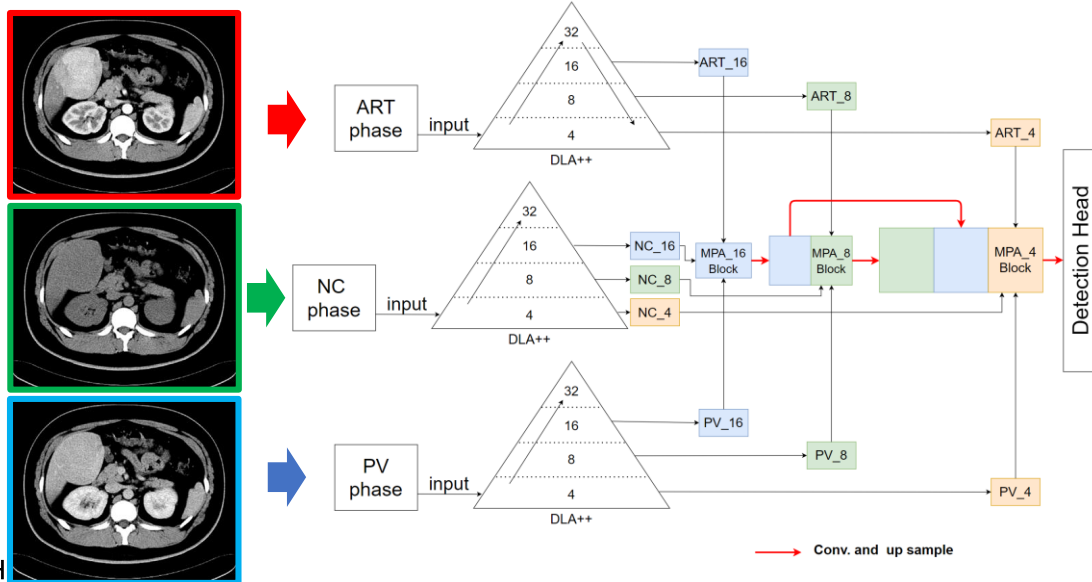
$$\hat{F}^s = F_{NC}^s \otimes \sigma(F_{NC, ART}^{S, s} + F_{NC, PV}^{S, s})$$

$$\hat{F}^2 = H(\hat{F}_{NC}^4, H(\hat{F}_{NC}^8, \hat{F}_{NC}^{16}), H(H(\hat{F}_{NC}^{16})))$$



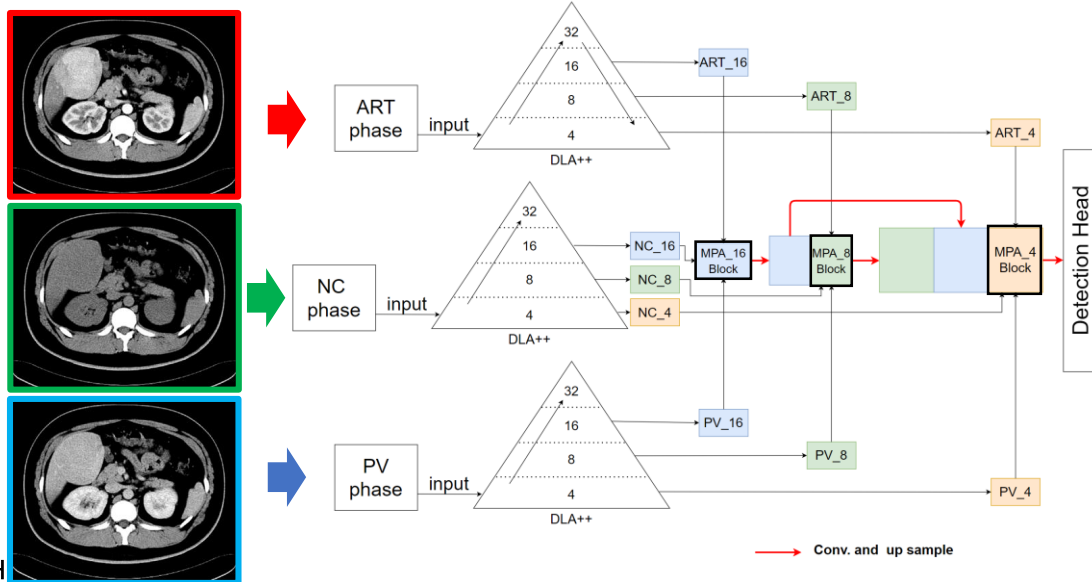


Flow of the our detection



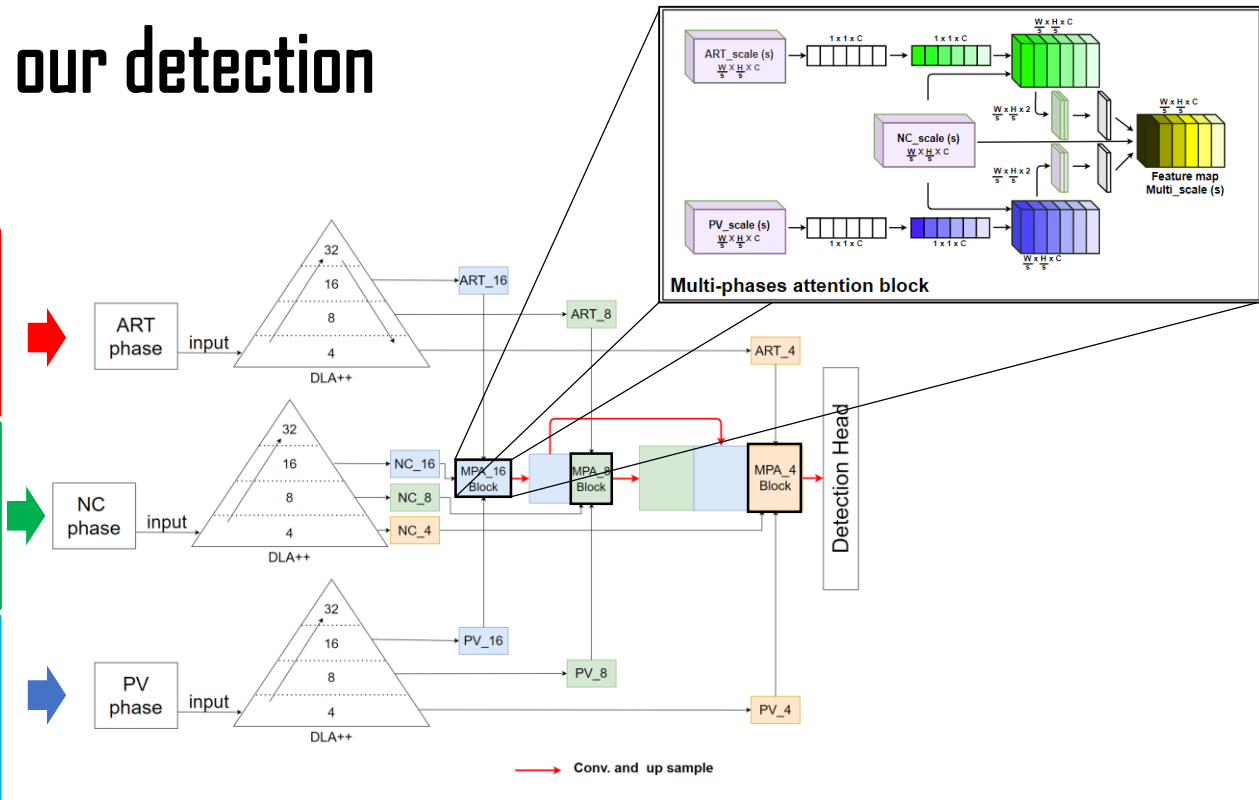
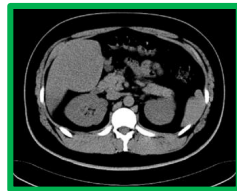
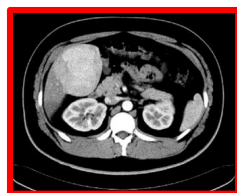


Flow of the our detection



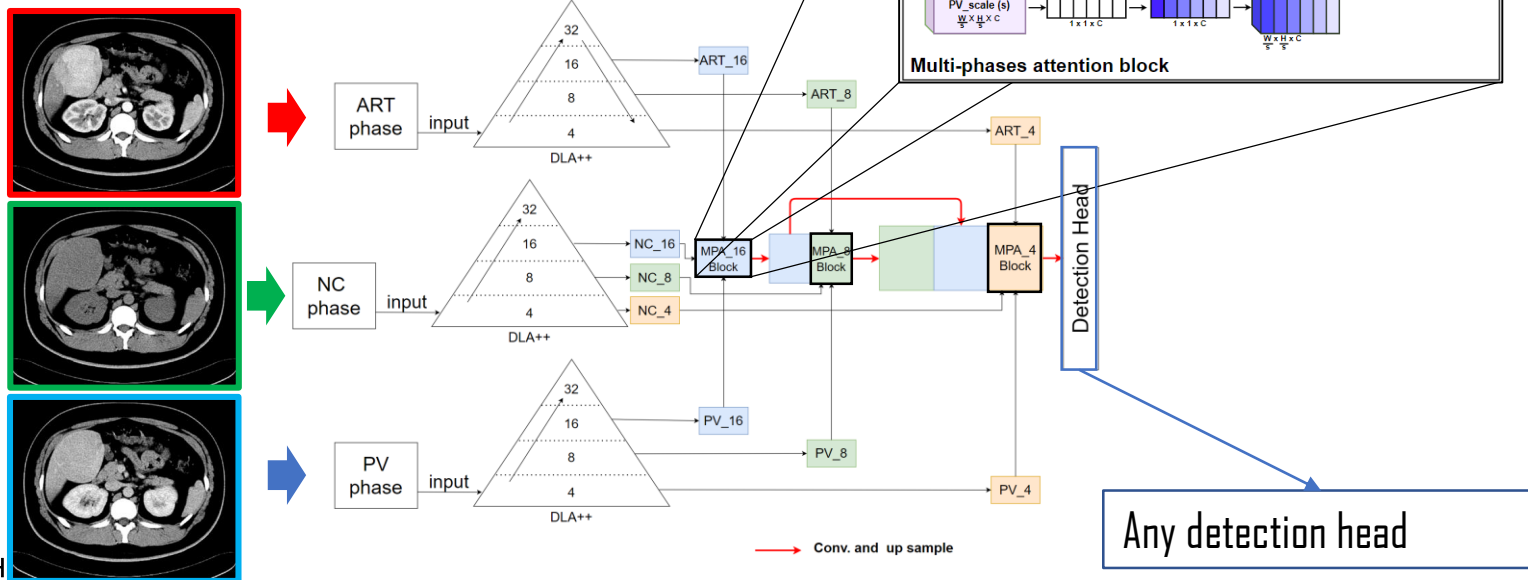


Flow of the our detection



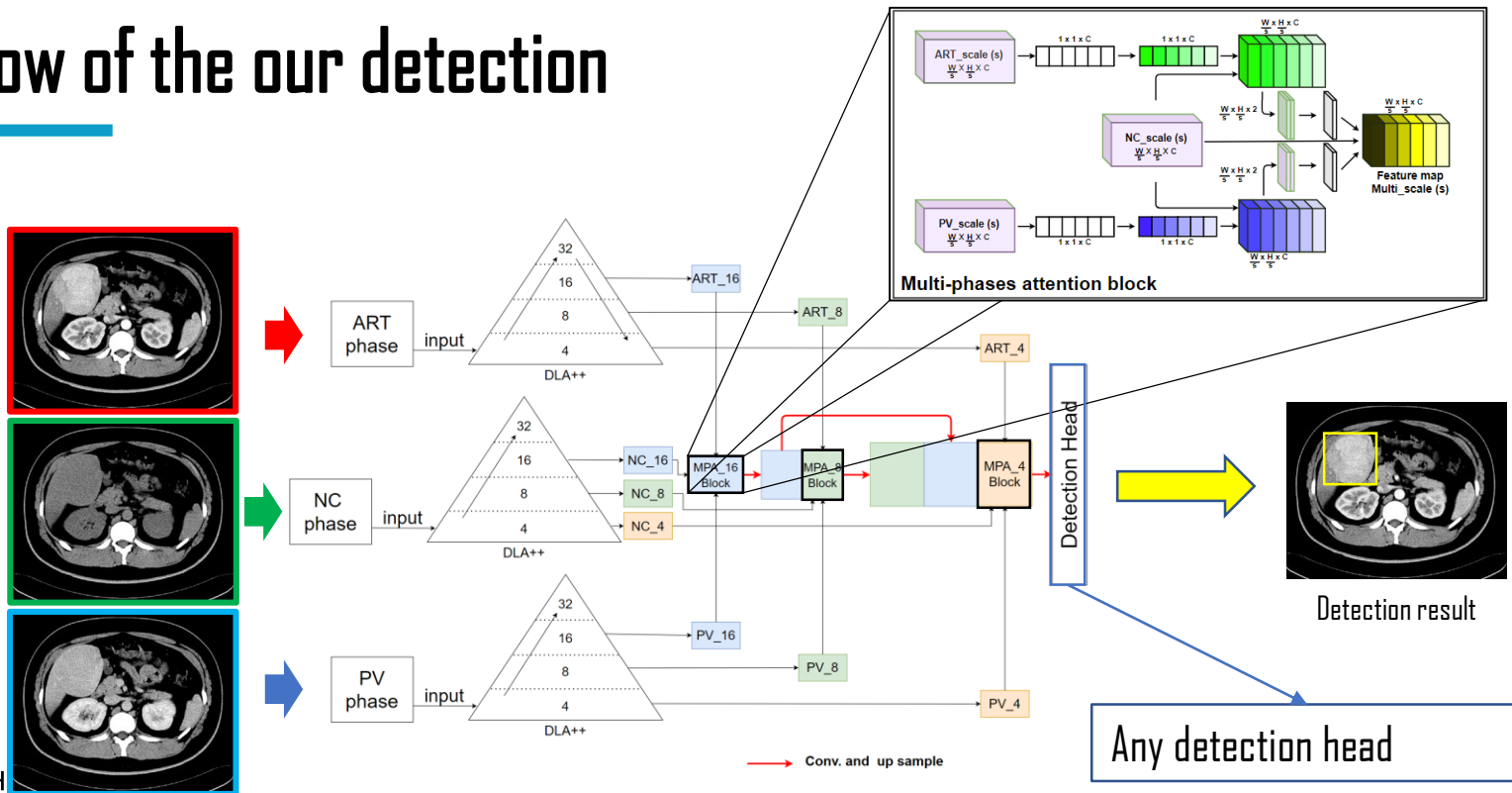


Flow of the our detection





Flow of the our detection





Comparison of detection result

Approach	Method	Sir Run Run Shaw Hospital			LiTS2017	
		AP@0.1	AP@0.5	AP@0.75	AP@0.5	AP@0.75
Anchor-based	SSD [3]	51.48±1.78	47.42±2.57	32.33±8.30	45.33±4.75	29.90±10.17
	Faster RCNN [2]	76.62±1.43	66.38±4.10	41.82±10.97	58.24±3.91	35.74±9.93
	GSSD [10]	63.57±2.09	57.81±1.99	46.25±4.88	50.21±4.81	34.52±10.04
	DeepLung [29]	80.33±4.47	68.01±9.91	47.44±9.19	70.29±4.79	45.41±7.89
	PixelLink [12]	83.08±4.32	69.94±9.25	-	-	-
	Liang et al [11]	88.45±2.46	77.06±5.85	-	-	-
	3DCE, 9 slices [30]	55.97±4.44	53.47±9.94	42.25±9.79	60.72±5.35	36.00±9.26
	3DCE, 27 slices [30]	81.84±1.22	68.09±1.70	47.60±4.78	69.22±4.90	38.72±8.91
	3DCE, 9 slices multi-phases [30]	92.41±1.22	83.68±3.78	59.48±5.35	-	-
Anchor-free	CornerNet [13]	84.79±2.92	72.48±4.76	49.54±7.33	64.56±5.01	42.73±9.13
	ExtremeNet [14]	88.30±4.13	75.52±3.30	56.91±5.93	66.87±5.77	45.98±6.90
	CenterNet [16]	90.32±1.55	81.07±3.89	53.29±6.01	73.55±4.21	45.31±7.27
	MSPA-DLA++ (single phase)	-	-	-	74.00±4.23	48.25±6.32
	MSPA-DLA++	94.02±0.98	84.26±3.02	60.08±5.16	-	-



The effectiveness of DLA++

Model	Backbone	Phase	AP@0.1	AP@0.5
S1	DLA [16]	Single phase	90.32±1.55	81.07±3.89
S2	DLA++	Single-phase	91.27±1.32	81.90±3.65
M1	DLA	Multi-phase	91.29±1.33	81.79±3.75
M2	DLA++	Multi-phase	91.81±1.40	82.07±3.51

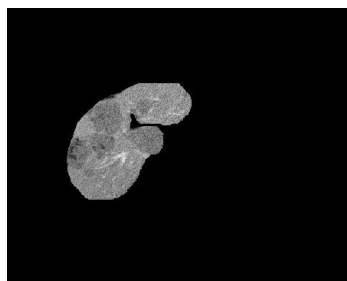


Ablation study

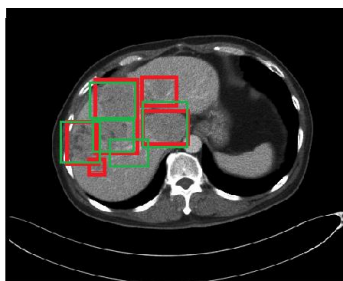
Model	Backbone	Phase	Multi-scales	PA	AP@0.1	AP@0.5
S2	DLA++ [31]	-	-	-	91.27 ± 1.32	81.90 ± 3.65
M2	DLA++	✓	-	-	91.81 ± 1.40	82.07 ± 3.51
M3	G-DLA++	✓	✓	-	92.30 ± 1.15	82.56 ± 3.38
M4	MA-DLA++	✓	-	✓	93.01 ± 1.03	82.72 ± 3.40
M5	MSPA-DLA++	✓	✓	✓	94.02 ± 0.98	84.26 ± 3.02



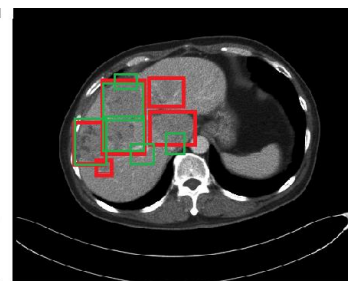
Visualization results



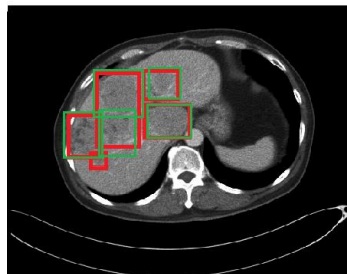
(a) Input image



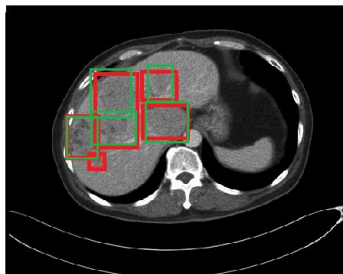
(b) Faster RCNN



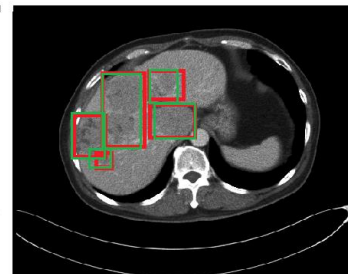
(c) SSD



(d) ExtremeNet



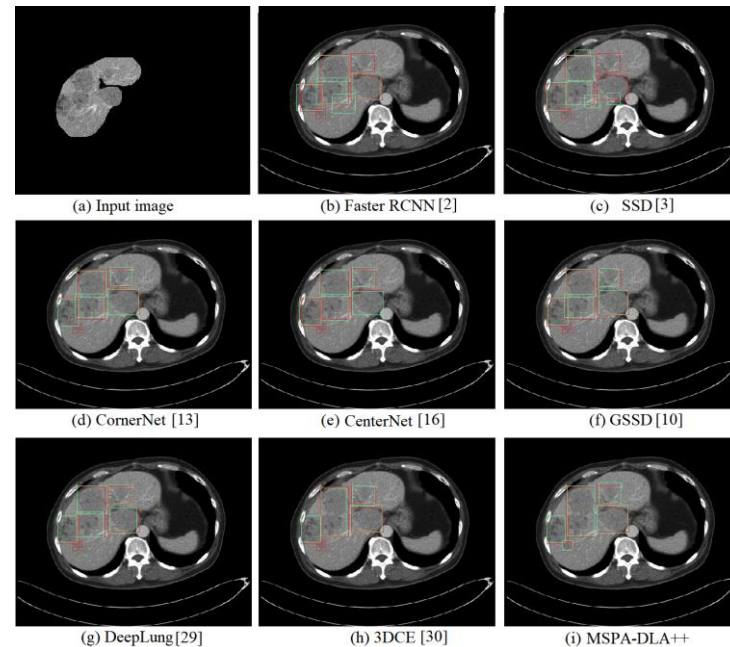
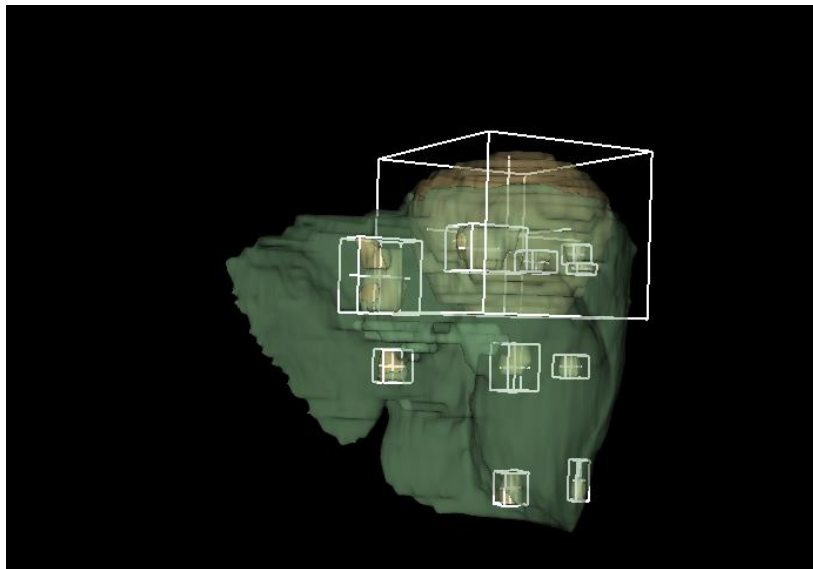
(e) CenterNet



(f) RDLA++



Visualization results



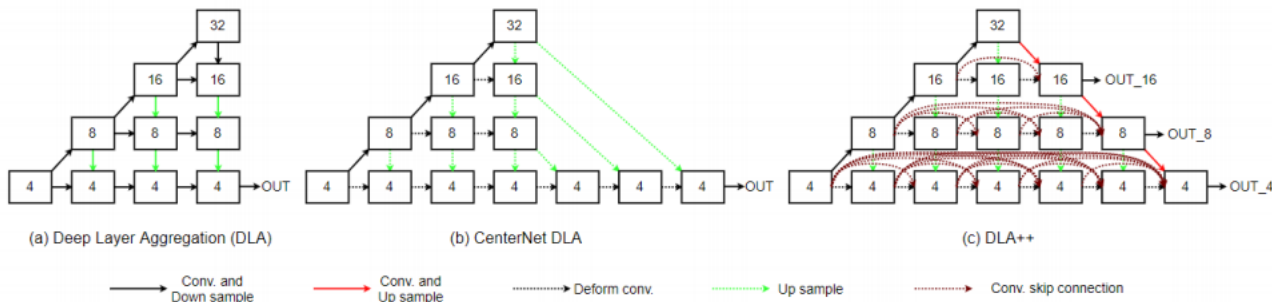
MED INFO 23

8 - 12 JULY 2023 | SYDNEY, AUSTRALIA

Thank you



DLA++



$$x_j^i = \begin{cases} H([x_j^{i-1}]), & j = 0 \\ H([U(x_{j-1}^{i+1}), [x_k^i]_{k=0}^{j-1}]), & 0 < j < J - ((i \times 2) + 1) \\ H([U(x_{j-2}^{i+1}), [x_k^i]_{k=0}^{j-1}]), & \text{otherwise} \end{cases}$$